Higher order approximations of the transmission and escape probability method for neutral particle transport in edge plasmas

Dingkang Zhang, J. Mandrekas, and W. M. Stacey
Fusion Research Center, Georgia Institute of Technology, Atlanta, Georgia 30332

(Received 4 February 2006; accepted 19 May 2006; published online 19 June 2006)

Higher order approximations, which take into account the effects of angular anisotropy, spatial nonuniformity and energy dependence of the distribution of neutral particles, have been developed and implemented to extend the range of validity of the transmission and escape probabilities (TEP) method for the calculation of neutral particle transport in plasmas. Comparisons with Monte Carlo calculations of model test problems and DIII-D [J. Luxon, Nucl. Fusion, **42**, 614 (2002)] *L*- and *H*-mode discharges show that these new extensions significantly improve the accuracy and extend the range of validity of the TEP methodology. © *2006 American Institute of Physics*.
[DOI: 10.1063/1.2212934]

I. INTRODUCTION

Neutral particles at the edge of magnetically confined plasmas can have a strong effect on plasma-wall interactions as well as on the properties and the performance of the core plasma. Therefore, computational tools for the simulation of neutral particle transport in plasmas are essential components of plasma edge simulations. The transmission and escape probability (TEP) method[1] is a deterministic and computationally fast technique for neutral transport simulations which can handle the geometric complexity encountered in realistic plasma edge configurations.

The TEP method has been successfully implemented into the GTNEUT code[2] which has undergone an extensive verification and validation process through benchmarks with Monte Carlo codes and comparison against experimental results.[3,4] However, these comparisons also revealed that certain simplifying assumptions in the original TEP methodology limited its accuracy and range of validity. These assumptions include: (1) the double P_0 (DP_0) approximation, which assumes the neutral angular fluxes are isotropic on both the inward and outward hemispheres and which is strictly valid only in short mean-free-path regions within which large charge-exchange/scattering rates isotropize the neutral distribution, (2) the uniform or "flat" collision source approximation, which assumes collided neutrals are uniformly distributed within each computational region and is strictly valid only in regions with long neutral mean-free path compared to the size of the region, and (3) the local ion temperature approximation, which assumes the average energy of neutrals within a region is equal to the local ion temperature and is valid if the characteristic ion temperature gradient scale length $L=T/|\nabla T|$ is larger than local neutral mean-free-path λ.

To address these issues and extend the accuracy and range of validity of the TEP methodology and the GTNEUT code, the original formulation has been extended by implementing the following improvements: First, the original DP_0 approximation has been extended to take into account linearly (DP_1) and quadratically (DP_2) anisotropic distributions of angular fluxes. Second, three approaches have been implemented and evaluated—subdivision into short mean-free-path regions, expansion of collision sources and intraregion diffusion calculation—to account for the nonuniformity of the collision source. In addition, spatial nonuniformities of the angular fluxes along the cell interfaces have been taken into account by expanding the neutral distribution function into a set of spatially linear representation functions. Finally, the average neutral energy (ANE) approximation, which assumes the average neutral energy within a region is the weighted average of the energies of neutrals entering from contiguous regions and of the energy of neutrals resulting from charge-exchanged ions within the region, has been developed and implemented into the GTNEUT code. The upgraded code is benchmarked against Monte Carlo for model problems designed to test the original assumptions and for realistic DIII-D plasmas.

This article is organized as follows: in Sec. II, the original TEP methodology is summarized. In Sec. III, the implementation of the DP_1 and DP_2 approximations is described. In Sec. IV, the effects of the collision source nonuniformity are addressed. The average neutral energy approximation is discussed in Sec. V. Sections VI and VII present benchmarking calculations with Monte Carlo for both simple model problems and realistic DIII-D plasmas. Finally, conclusions and discussions follow.

II. ORIGINAL TEP METHODOLOGY

The TEP methodology results from partitioning the domain of the problem into a large number of finite size regions and formulating a balance equation to calculate the neutral partial current crossing the interfaces bounding each region.[1] The partial current $\Gamma_{i,j}$ from region i to region j, can be expressed as

$$\Gamma_{i,j} = \sum_k T^i_{k,j}\Gamma_{k,i} + \sum_k \left(1 - \sum_l T^i_{k,l}\right) c_i P_i \Lambda_{ij} + S^i_{\text{ext}} P_i \Lambda_{ij}, \tag{1}$$

where $T^i_{k,j}$ is the first-flight transmission probability across region i from contiguous region k to contiguous region j, P_i

is the total escape probability from region i, $P_i\Lambda_{ij}$ is the directional escape probability from region i to region j, c_i is the charge exchange fraction, and S^i_{ext} is the total external volumetric neutral source in region i. A more detailed explanation of these terms is included in Refs. 1 and 2. The physical meaning of the pervious balance equation is clear: the first term on the right-hand side (rhs) represents neutrals entering from all contiguous regions which are directly transmitted into region j without collision within region i, the second term consists of all neutrals entering region i from all adjacent regions which will have one or more collision within region i and eventually escape into region j, and the third term is simply the contribution from any external volumetric sources such as recombination within region i.

The original TEP method was formulated under the following plausible assumptions: (1) double P_0 or DP_0 approximation, (2) flat collision source approximation, and (3) local ion temperature approximation. In the first approximation, neutral particles are assumed to be isotropically distributed over both the inward and outward hemispheres at each interface for the purpose of calculating the surface-to-surface transmission probabilities. Extensive comparisons with Monte Carlo calculations indicate that the DP_0 approximation is valid for short mean-free-path regions, where the neutral angular distribution is isotropized by charge exchange and elastic scattering collisions with the background plasma ions. However, in long mean-free-path regions, anisotropies may be introduced by the longer path lengths neutral traveling obliquely than perpendicular to the incident surface, in which case the DP_0 approximation leads to an underestimation of the uncollided flux transmitted to adjacent regions, and this anisotropy builds up at successive interfaces for uncollided particles.

In the second assumption, collision sources are assumed to be uniformly distributed within each computational region in the evaluation of the total and directional escape probabilities. This flat collision source approximation is reasonable as long as the neutral mean-free-path λ is longer than the characteristic dimension Δ of the computational region. However, for short mean-free-path regions, charge exchanged or elastically scattered neutral collisions are predominantly distributed close to the incident surfaces, resulting in a strongly nonuniform collision source. As a result, the flat collision source approximation leads to an overestimation of collided fluxes in the forward direction.

In the local ion temperature approximation, neutrals within a region are assigned an average energy equal to 3/2 the local ion temperature. The local ion temperature approximation is reasonable if the local background plasma ion temperature T changes slowly within a mean-free path, i.e., $\lambda/L<1$, where L is the characteristic ion temperature gradient scale length defined as $L=T/|\nabla \ln T|$. However, if this condition is not met, the uncollided neutrals entering a region will have energies characteristic of the region of their last collision, which can be very different from the local ion temperature.

III. ANISOTROPIC ANGULAR FLUXES

To extend the validity of the TEP methodology to cases with strong anisotropies, the neutral angular flux at the interface between regions i and j is expanded into a set of orthonormal angular representation functions:

$$\psi(\mathbf{r}_{ij},\mathbf{\Omega}) = \sum_n \Gamma^n_{i,j}\psi^n_{i,j}(\mathbf{r}_{ij},\mathbf{\Omega}), \tag{2}$$

where $\psi^n_{i,j}(\mathbf{r}_{ij},\mathbf{\Omega})$ are the expansion functions and $\Gamma^n_{i,j}$ are the nth expansion coefficients or the nth moment of partial current from region i to region j. This is a standard technique which has been used to deal with anisotropic neutron fluxes in fission reactors.[5,6] The angular expansion functions $\psi^n_{i,j}(\mathbf{r}_{ij},\mathbf{\Omega})$ are defined as[7,8]

$$\begin{aligned}
\psi^0_{i,j}(\mathbf{r}_{ij},\mathbf{\Omega}) &= \frac{1}{\pi S_{ij}},\\
\psi^1_{i,j}(\mathbf{r}_{ij},\mathbf{\Omega}) &= \frac{2}{\pi S_{ij}}\sin\theta_{ij}\sin\phi_{ij},\\
\psi^2_{i,j}(\mathbf{r}_{ij},\mathbf{\Omega}) &= \frac{3\sqrt{2}}{\pi S_{ij}}\sin\theta_{ij}\cos\phi_{ij} - 2\sqrt{2}\psi^0_{i,j}(\mathbf{r}_{ij},\mathbf{\Omega}),\\
\psi^3_{i,j}(\mathbf{r}_{ij},\mathbf{\Omega}) &= \frac{20}{\sqrt{17}\pi S_{ij}}\sin^2\theta_{ij} - \frac{2\sqrt{2}}{\sqrt{17}}\psi^2_{i,j}(\mathbf{r}_{ij},\mathbf{\Omega})\\
&\quad - \frac{15}{\sqrt{17}}\psi^0_{i,j}(\mathbf{r}_{ij},\mathbf{\Omega}),\\
\psi^4_{i,j}(\mathbf{r}_{ij},\mathbf{\Omega}) &= \frac{3\sqrt{34}}{\pi S_{ij}}\sin^2\theta_{ij}\sin^2\phi_{ij} - \frac{49}{10\sqrt{2}}\psi^3_{i,j}(\mathbf{r}_{ij},\mathbf{\Omega})\\
&\quad + \frac{3\sqrt{17}}{5}\psi^2_{i,j}(\mathbf{r}_{ij},\mathbf{\Omega}) - \frac{3\sqrt{34}}{4}\psi^0_{i,j}(\mathbf{r}_{ij},\mathbf{\Omega}),\\
\psi^5_{i,j}(\mathbf{r}_{ij},\mathbf{\Omega}) &= \frac{30}{\sqrt{11}\pi S_{ij}}\sin^2\theta_{ij}\sin\phi_{ij}\cos\phi_{ij}\\
&\quad - \frac{8}{\sqrt{11}}\psi^1_{i,j}(\mathbf{r}_{ij},\mathbf{\Omega}) - \frac{15}{\sqrt{17}}\psi^0_{i,j}(\mathbf{r}_{ij},\mathbf{\Omega}),
\end{aligned} \tag{3}$$

where S_{ij} represents the area of the interface between regions i and j, θ_{ij} is the polar angle of the direction $\mathbf{\Omega}$, ϕ_{ij} is the azimuthal angle. $\psi^0_{i,j}(\mathbf{r}_{ij},\mathbf{\Omega})$ represents the isotropic expansion function (DP_0); $\psi^1_{i,j}(\mathbf{r}_{ij},\mathbf{\Omega})$ and $\psi^2_{i,j}(\mathbf{r}_{ij},\mathbf{\Omega})$ represent the linearly anisotropic expansion function (DP_1); $\psi^3_{i,j}(\mathbf{r}_{ij},\mathbf{\Omega})$, $\psi^4_{i,j}(\mathbf{r}_{ij},\mathbf{\Omega})$, and $\psi^5_{i,j}(\mathbf{r}_{ij},\mathbf{\Omega})$ are the quadratically anisotropic expansion function (DP_2).

A rigorous derivation of the partial current equation for each moment or expansion coefficient can be found in Ref. 9. For completeness, the outline of the derivation is presented. The starting point is the integral form of the Boltzmann transport equation[10] for a domain D_i with boundary ∂D_i:

$$\psi(\mathbf{r},\mathbf{\Omega}) = \psi_{\text{in}}(\mathbf{r}_S,\mathbf{\Omega})\exp(-\Sigma_t|\mathbf{r}-\mathbf{r}_S|) + \int_0^{R_S} dl q(\mathbf{r}-l\mathbf{\Omega},\mathbf{\Omega})\exp(-\Sigma_t l), \tag{4}$$

where $\psi_{\text{in}}(\mathbf{r}_S,\mathbf{\Omega})$ is the incoming angular flux in direction $\mathbf{\Omega}$ at point $\mathbf{r}_S$ located on the boundary ∂D_i; R_S is the distance between points r and $\mathbf{r}_S$; Σ_t is the total macroscopic cross section (equal to the reciprocal of the neutral mean-free-path λ). Similarly, Σ_{cx} is the macroscopic charge exchange cross section; $q(\mathbf{r},\mathbf{\Omega})$ is the total volumetric source defined as

$$q(\mathbf{r},\mathbf{\Omega}) = \int_{4\pi} d\mathbf{\Omega}'\Sigma_{\text{cxtel}}(\mathbf{r},\mathbf{\Omega}'\rightarrow\mathbf{\Omega})\psi(\mathbf{r},\mathbf{\Omega}') + S_{\text{ext}}(\mathbf{r},\mathbf{\Omega}), \tag{5}$$

where $S_{\text{ext}}(\mathbf{r},\mathbf{\Omega})$ represents the external volumetric source such as recombination neutrals. "cxtel" denotes charge-exchange and elastic scattering.

Using Eq. (2) to expand the incoming flux in the first term of the rhs of Eq. (4) and then projecting both sides of Eq. (4) onto each expansion function, yields the partial current balance equation. The exiting current from region i to region j in moment n, $\Gamma_{i,j}^n$, can be expressed as the sum of the uncollided current moments transmitted from all the contiguous regions and the collided current moments emitted from the collision sources within the region, via transmission and escape probabilities, respectively,

$$\Gamma_{i,j}^n = \sum_{k,n'} T_{i,k\rightarrow j}^{n'\rightarrow n}\Gamma_{k,i}^{n'} + \sum_{k,n'}\left(\delta_{n'0} - \sum_l T_{i,k\rightarrow l}^{n'\rightarrow n}\right) \times \Gamma_{k,i}^{n'} c_i P_i \Lambda_{ij}^n + S_{\text{ext}}^i P_i \Lambda_{ij}^n, \tag{6}$$

In Eq. (6), $T_{i,k\rightarrow j}^{n'\rightarrow n}$ is the transmission probability from region k and moment n' to region j and moment n across region i, P_i is the total escape probability, $\Lambda_{i,j}^n$ is the directional escape probability from region i to region j in moment n, c_i is the charge-exchange fraction, S_{ext}^i represents the total external volumetric source in region i, and $\delta_{nn'}$ is the Kronecker delta. The physical meaning of Eq. (6) is clear: the first term in the rhs represents the contribution to the nth moment of the partial current of uncollided neutral incident current moments n' from all the contiguous regions k directly transmitted to region j without collision within region i, the second term represents the contribution to the nth moment of the partial current of incident neutrals entering from all adjacent regions k, having one or more collisions within region i and eventually exiting into region j, the last term is just the contribution from the external volumetric source.

The first-flight transmission probability $T_{i,k\rightarrow j}^{n'\rightarrow n}$ in two-dimensional (2D) geometry can be calculated from

$$T_{i,k\rightarrow j}^{n'\rightarrow n} = \pi S_{ij}\int_{S_{ij}} d\mathbf{r}_{ij}\int_{S_{ki}} d\mathbf{r}_{ki}\psi_{i,j}^n(\mathbf{r}_{ij},\mathbf{\Omega})\psi_{k,i}^{n'}(\mathbf{r}_{ki},\mathbf{\Omega}) \times \frac{\exp\left(-\frac{|\mathbf{r}_{ij}-\mathbf{r}_{ki}|}{\lambda}\right)}{|\mathbf{r}_{ij}-\mathbf{r}_{ki}|^2}(\mathbf{\Omega}\cdot\mathbf{n}_{ij})(\mathbf{\Omega}\cdot\mathbf{n}_{ki}), \tag{7}$$

where λ is the neutral mean-free path within region i, and $\mathbf{n}_{ij}$ is the normal at interface S_{ij}.

In addition to the DP_1 or DP_2 approximation, the flat collision source approximation, which assumes a spatially uniform distribution of collision sources in each computational region, is made to derive the neutral particle balance equation. Assuming the angular flux at an interface due to volumetric sources is isotropic, the interface current balance equation (6) can be further simplified as

$$\Gamma_{i,j}^n = \sum_{k,n'} T_{i,k\rightarrow j}^{n'\rightarrow n}\Gamma_{k,i}^{n'} + \sum_{k,n'}\left(\delta_{n',0} - \sum_l T_{i,k\rightarrow l}^{n'\rightarrow 0}\right) \times \Gamma_{k,i}^{n'} c_i P_i \Lambda_{ij}^0 \delta_{n0} + S_{\text{ext}}^i P_i \Lambda_{ij}^0 \delta_{n0}. \tag{8}$$

Realizing that collided fluxes are important for short mean-free-path regions, where collisions tend to isotropize the neutral angular distribution, neglect of the higher moments of collided fluxes is a good approximation.

IV. CORRECTION TO DIRECTIONAL ESCAPE PROBABILITIES

The flat collision source approximation assumes that neutral sources due to charge exchanged or scattered neutrals, which are responsible for the collided term in the balance equations of partial current moments, are uniformly distributed within each computational cell. Detailed comparisons with Monte Carlo indicate that the flat collision source assumption is a good approximation for long mean-free-path regions, when the neutral mean-free-path λ is comparable to or larger than the characteristic dimension of the computational region Δ. However, if the neutral mean-free path is very short compared to Δ, the charge-exchanged or elastic scattering sources are preferentially located near the incident surface. In this case the flat collision source approximation leads to an overprediction of collided neutrals leaving the region in the forward direction.

The most straightforward approach to address the effects of the collision source nonuniformity is to subdivide each short mean-free-path region into a number of subregions, in each of which collision sources can be treated as uniform. This approach is similar to the adaptive mesh refinement method and does not require modifying the TEP methodology. However, it results in a large coefficient matrix which increases the computer processing unit (CPU) and memory storage requirements.

Alternatively, expanding the collision source in terms of spatially dependent functions, an effective technique used for calculation of neutron transport in fission reactors with repeated geometric configurations,[6] can be employed to represent collision sources with strong nonuniformities. However, implementing this approach in the absence of the highly

symmetric configurations common in nuclear reactors requires the evaluation of computationally expensive volume-to-volume and surface-to-volume collision probability integrals.

Finally, as the nonuniformity of the collision source becomes an issue only in cases where the neutral mean-free path is short compared to the cell dimension, i.e. $\lambda/\Delta \ll 1$, diffusion theory can be used to treat neutral transport within such regions and derive directional escape probabilities.

The first step in this approach is to break the problem into several relatively simple problems, each with a flux incident from only one of its sides. The directional escape problem can be decomposed accurately into a set of nonuniform source diffusion problems within each short mean-free-path region.

$$-\nabla \cdot D \nabla \phi(\mathbf{r}) + \Sigma_a \phi(\mathbf{r}) = S_{j,i}(\mathbf{r}), \tag{9}$$

with vacuum boundary conditions:

$$\frac{\phi(\mathbf{r})}{4} + \frac{\mathbf{n}_{ij} \cdot D \nabla \phi(\mathbf{r})}{2} = 0, \tag{10}$$

where $\phi(\mathbf{r})$ is the neutral scalar flux at point $\mathbf{r}$, D is the diffusion coefficient[8] defined as

$$D = \frac{1}{3(\Sigma_t - \bar{\mu}\Sigma_{\mathrm{cx}})}, \tag{11}$$

where $\bar{\mu}$ is the average cosine of the scattering angle, $\Sigma_a = \Sigma_t - \Sigma_{\mathrm{cx}}$ is the macroscopic ionization cross section, $\mathbf{n}_{ij}$ is the out normal at the interface between region i and region j, and $S_{j,i}(\mathbf{r})$ is the first collision source[11] associated with a flux injected from region j into region i. All secondary collision neutral sources are implicitly included in the fixed source diffusion equation (9). As a result, the nonuniformity of both the first and secondary collision neutral sources is taken into account.

Analytical solutions to Eq. (9) can only be found for rather idealized cases with regular geometries and homogeneous background plasmas. However, such cases rarely exist in realistic plasmas, where numerical evaluation is generally necessary. Among possible numerical methods of solving the fixed source diffusion equation with vacuum boundary conditions, the finite element method[8] is the most suitable for problems with geometric complexity and can be easily updated to the higher order approximations. The variational functional[8] of the diffusion equation with vacuum boundary conditions can be expressed as

$$F[\phi] = \int_{D_i} d\mathbf{r}\{D(\nabla\phi)^2 + \Sigma_a\phi^2 - 2\phi S_{j,i}\} + \frac{1}{2}\int_{\partial D_i} \phi^2 dS. \tag{12}$$

In this equation, D_i represents the entire domain of region i, and ∂D_i its boundary. The requirement that the variational functional (12) is stationary is equivalent to the original diffusion equation, but the variational treatment leads to a significant improvement in overall efficiency and versatility of numerical approximations over the original differential equation as we can see from the following numerical implementation.

The first step in the variational diffusion treatment of directional escape probabilities is to divide a short mean-free-path region into a set of nonoverlapping subregions. The neutral flux within the region can be expressed in terms of piecewise linear representation functions:

$$\phi(\mathbf{r}) = \sum_{n=1}^{N} \phi_n h_n(\mathbf{r}), \tag{13}$$

where $h_n(\mathbf{r})$ are piecewise linear representation functions and ϕ_n are expansion coefficients. The form of $h_n(\mathbf{r})$ depends on the geometric configuration of each subregion, and the details of how to construct these representation functions can be found in Ref. 8.

The next step is to substitute the representation functions into the variational functional and require it to be stationary. Then the expansion coefficients ϕ_n can be determined from the solution to the following linear system:

$$A\Phi = S, \tag{14}$$

where Φ is the coefficient vector, $\Phi = \{\phi_1, \phi_1, \ldots, \phi_N\}^T$, the matrix A is defined as

$$A = \int_{D_i} d\mathbf{r}[D \nabla \mathbf{H} \cdot \nabla \mathbf{H}^T + \Sigma_a \mathbf{H}\mathbf{H}^T] + \frac{1}{2}\oint_{\partial D_i} \mathbf{H}\mathbf{H}^T dS \tag{15}$$

and the source vector

$$\mathbf{S} = \int_{D_i} d\mathbf{r}\mathbf{H} S_{ji} \tag{16}$$

and

$$\mathbf{H} = \{h_1(\mathbf{r}), h_2(\mathbf{r}), \ldots, h_N(\mathbf{r})\}^T. \tag{17}$$

Several properties of matrix A can be exploited to achieve high computational efficiency: the representation functions $h_n(\mathbf{r})$ are locally defined, and consequently, matrix A is sparse and we only need to calculate and store all the nonzero elements. Matrix A depends only on the geometric and background plasma properties. As a result, it needs to be evaluated only once for calculating directional escape probabilities associated with neutrals incoming from different interfaces.

With the linear system solved, the partial current can be easily obtained from Fick's law, i.e., $\mathbf{J} = -D\nabla\phi(\mathbf{r})$. Obviously, the total escape probability can be calculated as the ratio of the total current exiting from the region to the neutrals born within the region, whereas the directional escape probabilities are just the fraction of the neutral current exiting from a specific bounding surface. As a result, the total and directional escape probabilities associated with a flux imposed on interface ∂D_{ji} can be represented as

$$P_i^j = \frac{\oint_{\partial D_i} dS(\mathbf{n}_+ \cdot \mathbf{J}_+(\mathbf{r}))}{\int_{D_i} S_{ji}(\mathbf{r}) d\mathbf{r}}, \tag{18}$$

and

$$\Lambda_{i,k}^j = \frac{\int_{\partial D_{ik}} dS(\mathbf{n}_+ \cdot \mathbf{J}_+(\mathbf{r}))}{\oint_{\partial D_{ik}} dS(\mathbf{n}_+ \cdot \mathbf{J}_+(\mathbf{r}))}, \tag{19}$$

where the total escape probability P_i^j is the probability that the first charge-exchanged neutrals, originally entering region i from region j, have zero or more collisions within region i and finally escape from region i. The directional escape probability $\Lambda_{i,k}^j$ is the probability that neutrals escaping from region i, associated with the neutrals originally entering region i from region j, escape into region k. $\mathbf{n}_+$ represents the outward normal at the boundary, and $\mathbf{J}_+(\mathbf{r})$ is the outward partial current.

V. AVERAGE NEUTRAL ENERGY (ANE) APPROXIMATION

The original TEP methodology is based on the local ion temperature (LIT) approximation, which assumes the energy of neutrals in each computational region is equal to the 3/2 local ion temperature. If neutrals originate from boundaries, their energies are set by the corresponding boundary models (such as albedo, mirror, or reflection from material walls). Extensive tests against Monte Carlo calculations have shown this LIT approximation to be accurate for regions with a short mean-free path compared to the background ion temperature scale length $L_T = T|\nabla \ln T|^{-1}$. However, if the neutral mean-free path is much longer than L_T, the neutral flux from a region is primarily due to uncollided neutrals, which could have very different energy from the local charge-exchanged neutrals.

A two-group treatment of the energy dependence has been already implemented in the GTNEUT code to treat the energy dependence of wall reflected neutrals.[4] In that approach, the neutral population was divided into two distinct energy groups: a slow energy group consisting of Franck-Condon atoms, and a fast energy group consisting of collided neutrals in thermal equilibrium with the local plasma ion populations. However, the two-group approximation may not be sufficient to represent the neutral energy dependence when background plasmas are characterized by strong gradients in the background ion temperature. Although this issue could be addressed by a full multigroup implementation, it would require time consuming evaluation of probability matrices for each energy group. The ANE approximation introduced in this section is intended to provide a more computationally efficient approximation.

Neutral energy can affect neutral transport in two ways: First, the reaction rates of most atomic processes—and consequently the associated neutral mean-free path—depend on neutral energy. Second, the determination of the neutral densities from the angular flux and the interface currents depends strongly on their assumed energies. The first effect is not important for long mean-free-path regions, in which the attenuation is negligible ($e^{-L/\lambda} \approx 1$). Consequently, an error in the neutral energy would not introduce a big error in neutral fluxes. The second effect becomes dominant for long mean-free-path regions. Even if the neutral flux ψ is not affected by the neutral energy E, the neutral density n is inversely proportional to the square root of E, i.e., $n = \psi/v \propto \psi/\sqrt{E}$. However, this effect can be easily corrected if the average neutral velocity or equivalently energy is known.

The outgoing neutral partial current from region i into region j, according to the particle balance equation (4), can be separated into several distinct energy components: uncollided neutral partial current $\Sigma_{n'} T_{i,k\to j}^{n'\to 0} \Gamma_{k,i}^{n'}$, directly transmitted from an adjacent region k into region j through region i and having an average energy $\bar{E}_{ki}$; and collision and recombination neutral currents $\Gamma_{i,j}^{c,0} = \Sigma_{k,n'} \Gamma_{k,i}^{n'} (\delta_{n'0} - \Sigma_l T_{i,k\to l}^{n'\to 0}) c_i^k P_i^k \Lambda_{i,j}^k + S_{\text{ext}}^i P_i \Lambda_{ij}$ and having an average neutral energy which is in thermal equilibrium with the local ion temperature T_i. The average neutral energy for neutrals from region i into region j can be expressed as

$$\bar{E}_{ij} = \frac{\sum_{k,n} T_{i,k\to j}^{n\to 0} \Gamma_{k,i}^n \bar{E}_{ki} + \Gamma_{i,j}^{c,0} T_i}{\sum_{k,n} T_{i,k\to j}^{n\to 0} \Gamma_{k,i}^n + \Gamma_{i,j}^{c,0}}. \tag{20}$$

Essentially, the ANE approximation calculates the average energy of the neutrals crossing an interface as a weighted average of the average energies of neutrals entering the region from contiguous regions and the average energies (3/2 the local ion temperature) of neutrals charge exchanging in the region. For short mean-free-path regions where collided neutrals are dominant, or in cases where the background ion temperature changes slowly, $\bar{E}_{ki} \approx 3/2 T_i$, i.e., the ANE approximation reduces to the local ion temperature approximation.

In Eq. (20), the average energy for neutrals crossing an interface is coupled to the average energies of all neutrals entering from all the contiguous regions. The neutral transport equation can be solved by an iterative process:

(1) Assume $\bar{E}_{ij} = 3/2 T_i$ (the local ion temperature assumption);
(2) calculate the neutral mean-free-path, transmission and escape probabilities, and solve the linear system to determine the interface currents;
(3) calculate the collided and uncollided fluxes from the interface currents;
(4) use Eq. (20) to update the average neutral energy $\bar{E}_{ij}$;
(5) repeat steps 2-4 until convergence, which is determined by the maximum fractional change of $\bar{E}_{ij}$ from the previous iteration; and
(6) calculate the final neutral densities and the ionization rates.

As the numerical evaluation of the various transmission probabilities involves the computation of multidimensional

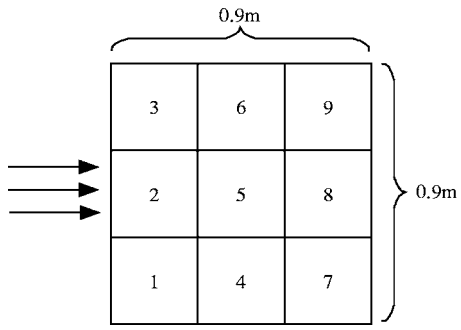

FIG. 1. Geometric configuration of a 2D nine-region model problem.

integrals, direct full iterations are computationally expensive. However, separating the iterations in the following two levels can achieve both computational efficiency and accuracy: partial iterations in step 4 without correcting for transport effects, and full iterations in steps 2–4 with reevaluation of the transmission and escape probabilities. Extensive benchmarks show that convergence can be obtained after 2 or 3 full iterations.[9]

VI. MODEL PROBLEM CALCULATION OF THE NEW APPROXIMATIONS

The extensions to the TEP methodology outlined in Sec. V have been implemented into the GTNEUT neutral transport code.[12] The validity of each single new approximation has been demonstrated by extensive comparisons with Monte Carlo calculations[7,9,12] for specially designed problems. In this section, the combined effects of all the new extensions are presented.

The model problem consists of nine identical squares with a length of 0.3 m. The geometric configuration and cell arrangement is illustrated in Fig. 1. Vacuum boundary conditions are assumed on the four external boundaries. An isotropic, uniform and unit strength neutral flux with an energy of 10 eV is injected at the left boundary of cell 2.

A. Short mean-free-path case

In the first case, the background ion temperature, electron temperature, ion and electron density vary linearly from 10 eV, 6 eV, 1.7×10^{19} m^{-3} in cells (cells 1, 2, and 3) adjacent to the left boundary to 100 eV, 10 eV, 2.7×10^{19} m^{-3} in cells (cells 7, 8, and 9) adjacent to the right boundary, respectively. The resulting charge exchange fraction c_i varies from 0.88 to 0.92, and the mean-free path varies from 0.085 to 0.091 m, which is shorter than the characteristic dimension of all regions.

The neutral mean-free path is much shorter than the characteristic ion temperature gradient length. The effects of this fact are twofold. On the one hand, it is expected that collided neutrals are preferentially distributed close to the incident surface. As a result, the GTNEUT code with the diffusion approximation should improve the accuracy of the TEP method. On the other hand, neutrals entering into a region predominately consist of charge-exchanged or scattered neutrals from the previous computational region. Consequently, the DP_0 and local ion temperature approximations should sufficiently represent the neutral energy and angular distributions, and the DP1 and average neutral energy approximations should not further improve the accuracy.

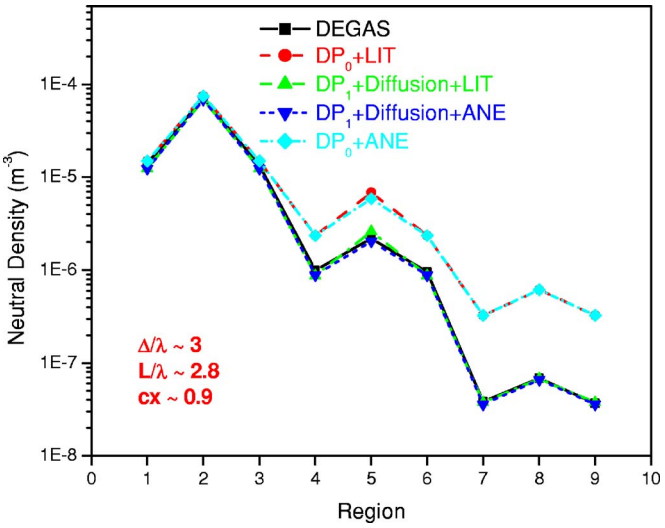

FIG. 2. (Color online) Comparison of DEGAS and GTNEUT for the shorter mean-free-path case.

The results of the GTNEUT and DEGAS[13] predictions are shown in Fig. 2, in which the five curves correspond to calculations of the Monte Carlo (labeled as DEGAS), GTNEUT with various approximations. It is clear that the calculation of GTNEUT with the flat collision source approximation significantly overestimates neutral densities for regions 4–9, whereas GTNEUT with corrections to directional escape probabilities using the diffusion approximation agrees very well with the DEGAS simulations. Because of the dominance of collided neutrals for all of the computational regions, there is no obvious improvement in accuracy either for the DP_1 or average neutral energy approximation. The comparison of the average neutral temperatures computed by the LIT and ANE approximations with the DEGAS calculations is shown in Table I, from which it is clear that the average neutral temperature is quite close to the local ion temperature in the same region. As a result, the LIT approximation can sufficiently represent the neutral energy distribution.

TABLE I. Comparison of the average neutral temperatures computed by different approximations for the shorter mean-free-path case (eV).

Region	LIT	ANE	DEGAS
1	10	10.5	10.7
2	10	10.7	10.3
3	10	10.5	10.7
4	55	47.1	40.6
5	55	47.2	38.5
6	55	47.1	40.1
7	100	91.0	84.3
8	100	91.7	84.5
9	100	91.0	85.5

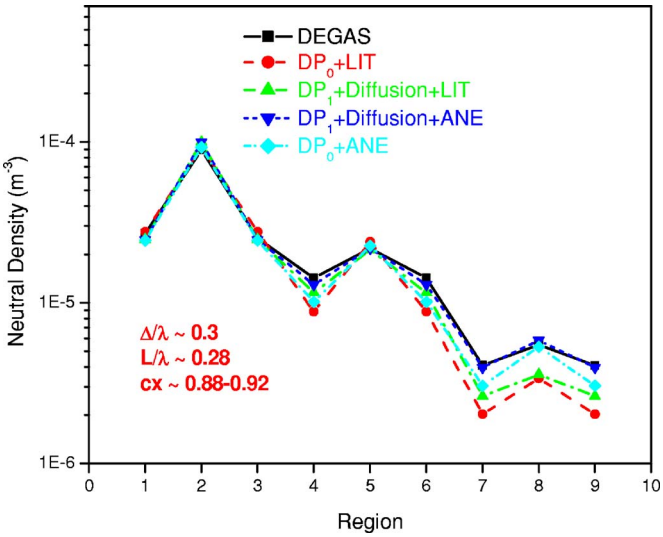

FIG. 3. (Color online) Comparison of DEGAS and GTNEUT for the longer mean-free-path case.

B. Long mean-free-path case

In the second case, the background ion temperature, electron temperature remain the same as in the previous case, whereas ion density and electron density are adjusted to be an order of magnitude lower than the first case, i.e., they vary linearly from 1.7×10^{18} m^{-3} in cells (1, 2, and 3) adjacent to the left boundary to 2.7×10^{18} m^{-3} in cells (7, 8, and 9) adjacent to the right boundary, respectively. The resulting charge exchange fraction c_i varies from 0.88 to 0.92, and the mean-free path varies from 0.85 to 0.94 m, which is longer than the characteristic dimension of all regions.

The comparison of the two codes with various approximations is shown in Fig. 3. As the neutral mean-free path is longer than the characteristic grid dimension, the DP_0 approximation, as discussed in Sec. II, overestimates neutral densities in cells away from the source. As the neutral mean-free path is also much longer than the characteristic ion temperature gradient length L, the neutral flux exiting across an interface consists predominantly of the uncollided neutrals from the adjacent regions, and therefore, the local ion temperature approximation, by which the local ion temperature is assigned to uncollided neutrals, is a poor approximation. For instance, all neutrals from regions 5 to 8 are assigned 55 eV by the local ion temperature approximation, but in reality, most of neutrals are directly transmitted from region 2 with an energy of 10 eV. As a result, the local ion temperature approximation leads to a significant underprediction of the neutral density in cell 8, as it overestimates the neutral energy. The same thing is true for regions 7 and 9 as it can be easily seen from Fig. 3. If the average neutral energy and the DP_1 approximations, as well as corrections to the nonuniformity of collided neutrals and angular fluxes, are made, the GTNEUT results agree very well with those predicted by Monte Carlo. By checking the results, it is found neutrals from regions 5 to 8 are assigned 25 eV, which is significantly lower than the local ion temperature in region 5. It also should be mentioned that the GTNEUT calculation with the average neutral energy approximation converges after 2 or 3 iterations, where the convergence criterion is the maximum change of average neutral energies from the previous iteration is less than 1%. To evaluate the effectiveness of the new ANE approximation and its improvement over the LIT model, the average neutral energies calculated by the two approximations are shown in Table II and compared against the predictions of the DEGAS code. It can be seen the predictions of the ANE approximation are much closer to the DEGAS results whereas the neutral energies predicted with the LTI approximation are much higher.

TABLE II. Comparison of the average neutral temperature computed by the different approximations for the longer mean-free-path case (eV).

Region	LIT	ANE	DEGAS
1	10	14.0	13.4
2	10	14.0	11.5
3	10	14.0	13.4
4	55	27.7	22.8
5	55	27.8	22.5
6	55	27.7	23.5
7	100	37.0	36.9
8	100	35.2	38.1
9	100	37.0	38.1

VII. NEUTRAL TRANSPORT SIMULATIONS FOR DIII-D PLASMAS

In this section, as a further, practical verification and validation step, the simulations of neutral densities in the DIII-D tokamak reported in Ref. 4 are repeated with the upgraded code. As in Ref. 4, two DIII-D discharges are considered—an *L* mode and an *H* mode—and the predictions of our simulations are compared with the Monte Carlo code DEGAS and the measured neutral densities.

A. *L*-mode case

The geometric configuration of the *L*-mode DIII-D discharge 96740 at 2250 ms is shown in Fig. 4. The domain of interest is divided into 182 regions, within each of which the

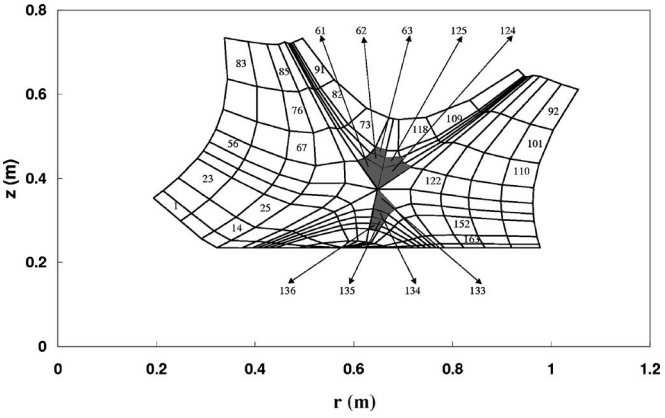

FIG. 4. Geometric model for the analysis of the DIII-D *L*-mode discharge 97640 at 2250 ms.

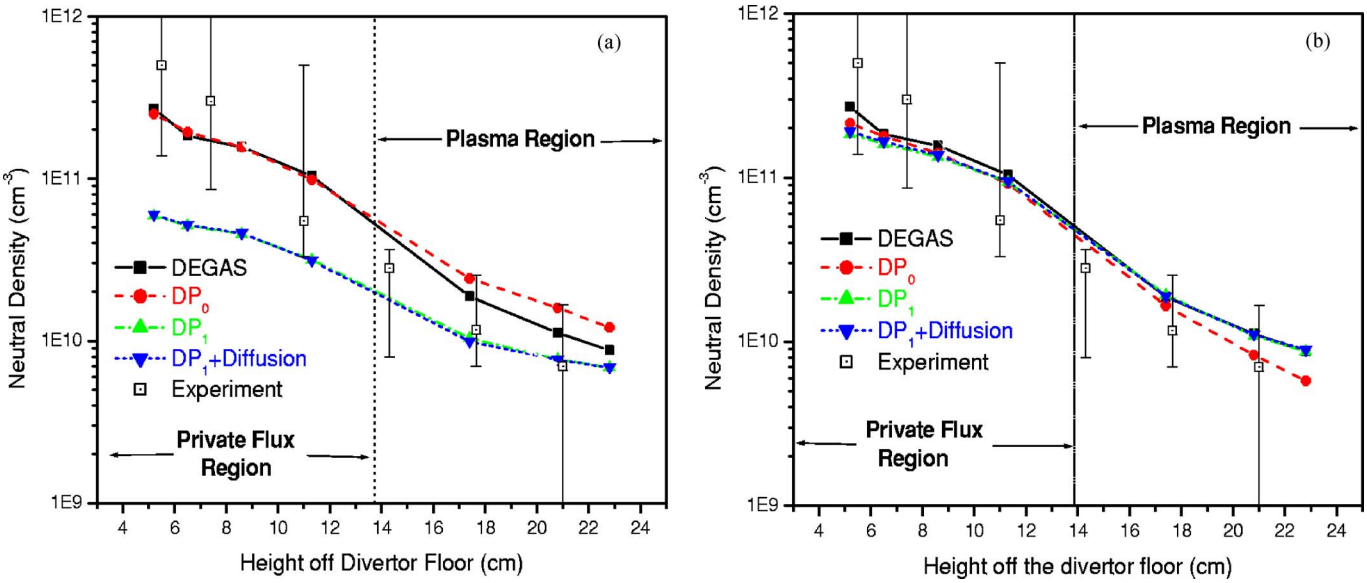

FIG. 5. (Color online) Comparison of GTNEUT and DEGAS simulations for the analysis of the DIII-D *L*-mode discharge 97640 at 2250 ms. (a) Local ion temperature approximation; (b) average neutral energy approximation.

background plasma properties can be approximately treated as uniform. The X point is located 13.8 cm above the divertor floor. The shaded regions in Fig. 4 represent the location where neutral densities were measured.[14] Cells 133–136 are located at the private flux region, whereas cells 61–63, 124, and 125 are located above the X point. The problem is bounded by carbon walls except for the top boundaries, which are treated as albedo boundaries.[1] Recycling sources are imposed on the bottom boundary of regions 1–10 and 172–181 which correspond to the location of the divertor plates. Plasma densities and temperatures vary from 3.1×10^{17} to 3.4×10^{19} m^{-3} and from 2.3 to 180 eV, respectively. The typical neutral mean-free path and the charge exchange fraction are in the range of 0.035–4.5 m and 0.52–1, respectively.

The reflection model described in Ref. 4 is used in this calculation. Recycled particles are categorized into two groups according to the particle-surface interaction processes: backscattering and desorption. In the former process, a neutral is recoiled back with a significant fraction of the impact energy after suffering a few elastic collisions with the target material. These energetic atoms are assumed to have a cosine current distribution. In the latter process, neutral particles are implanted in the near surface region, where they will reach thermal equilibrium with the wall material and subsequently be released as thermal molecules. As molecular transport is not included in the current version of the GTNEUT code, it is assumed that neutral molecules, released after coming into thermal equilibrium with wall materials, are immediately broken up as Frank-Condon atoms with energy of a few electron volts. DEGAS is also run without the molecule transport.

To assess the validity and effectiveness of the newly implemented ANE approximation described in Sec. V, two sets of GTNEUT simulations were carried out: in the first, the original local ion temperature assumption was used whereas the second set was performed under the ANE approximation. In each of these two cases, the various options for handling anisotropies and source nonuniformities described in the previous sections were exercised. The results of these simulations are shown in Figs. 5(a) (local ion temperature approximation) and 5(b) (ANE approximation), where the neutral densities predicted by the various GTNEUT simulations are plotted versus the height off the divertor floor. In each plot, the predictions of the DEGAS code as well as the measured neutral densities with their error bars are also shown.

From Fig. 5(a), it can be seen that in the case of the LIT approximation, the GTNEUT code with the DP_0 approximation (i.e., the original code used in Ref. 4) agrees very well with the DEGAS simulations in the private flux region, but it overpredicts the neutral densities by as much as 40% compared to DEGAS in the main plasma region. The GTNEUT code with the higher order approximations (the DP_1 approximation and the diffusion theory-corrected escape probabilities accounting for nonuniform collided neutral sources) underpredicts results by 30–300% compared to the Monte Carlo calculations. There is no significant difference between the calculations of GTNEUT with and without the diffusion theory-corrected escape probabilities, as expected as the mean-free path is comparable to the computational region dimension.

The disagreement of the GTNEUT predictions using the higher order approximations with DEGAS is attributed to the local ion temperature approximation, which is not valid for long mean-free-path regions. In such a situation the neutral mean-free path is much larger than the characteristic dimension for each computational region whereas the uncollided flux is about an order of magnitude higher than the collided flux at each interface. As a result, a significant fraction of the neutrals in the shaded regions are directly transmitted from the divertor floor with Franck-Condon energies of a few electron volts, whereas, under the LIT approximation used in

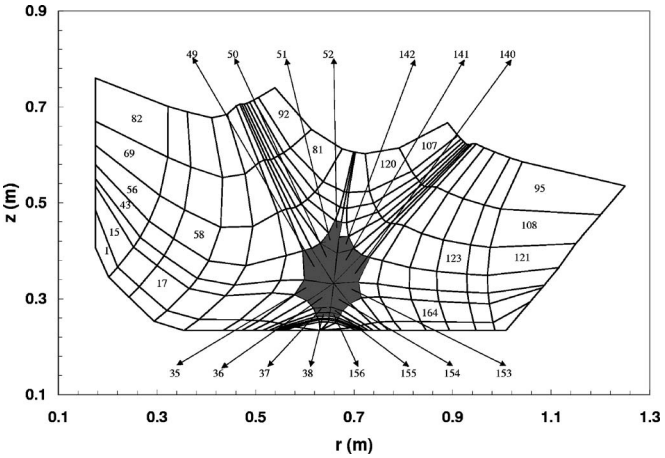

FIG. 6. Geometric model for the analysis of the DIII-D *H*-mode discharge 96747 at 3940 ms.

these simulations, they are assigned energies equal to the significantly higher local ion temperature.

In the case of the ANE approximation in Fig. 5(b), it can be seen that the simulation with the isotropic angular distribution assumption (DP_0) is in excellent agreement with DEGAS in the private flux region whereas it underpredicts the neutral densities in the main plasma region, as the DP_0 approximation leads to an under-prediction of transmission probabilities when the mean-free path is comparable to the computational region dimension. The simulation with the linearly anisotropic correction to the angular distribution (DP_1) is in excellent agreement with Monte Carlo for the entire region of interest. It should be also noted that, in this case, the diffusion correction to the directional escape probabilities is not significant due to the relatively large mean-free path of the neutrals.

B. *H*-mode case

The geometric model for the *H*-mode DIII-D discharge 96747 at 3940 ms is shown in Fig. 6. In this case, the X point is located 10.6 cm above the divertor floor. The problem consists of 188 regions. The shaded regions in Fig. 6 represent the location where the neutral densities were measured.[4] Cells 35–38 and 153–156 are located at the private flux region, cells 49–52 and 140–142 are located above the X point.

The external neutral sources are applied at the bottom boundary of regions 1–14 and 175–188, which correspond to the location of the divertor plates. Both the background plasma densities and temperatures are higher than those in the *L*-mode discharge. For example, the electron temperature varies from 3.8 to 59 eV in the private flux region and from 100 to 430 eV inside the separatrix, and ion temperature is in the range 57–218 eV in the private flux region and in the range 120–600 eV in the main plasma region. As a consequence, the neutral mean-free path varies from 0.7 to 26 m outside the separatrix and from 0.06 to 0.5 m in the plasma region, but it is much longer than the grid size for regions both outside and inside the separatrix, as in the *L*-mode case.

Two sets of GTNEUT simulations are presented, corresponding to the LIT [Fig. 7(a)] and ANE [Fig. 7(b)] treatments of the neutral energy. The LIT approximation fails in this case, as expected, in long mean-free-path regions.

In Fig. 7(b), the GTNEUT predictions using the ANE approximation are presented and compared with DEGAS. It can be seen that the agreement between the two codes is very good throughout the region. In particular, the case with the anisotropy corrections (DP1) with and without the diffusion corrections to the directional escape probabilities is in excellent agreement with Monte Carlo.

In both sets of simulations, the predictions of the two codes are in reasonable agreement with the experimental results. The observed disagreement between simulation and ex-

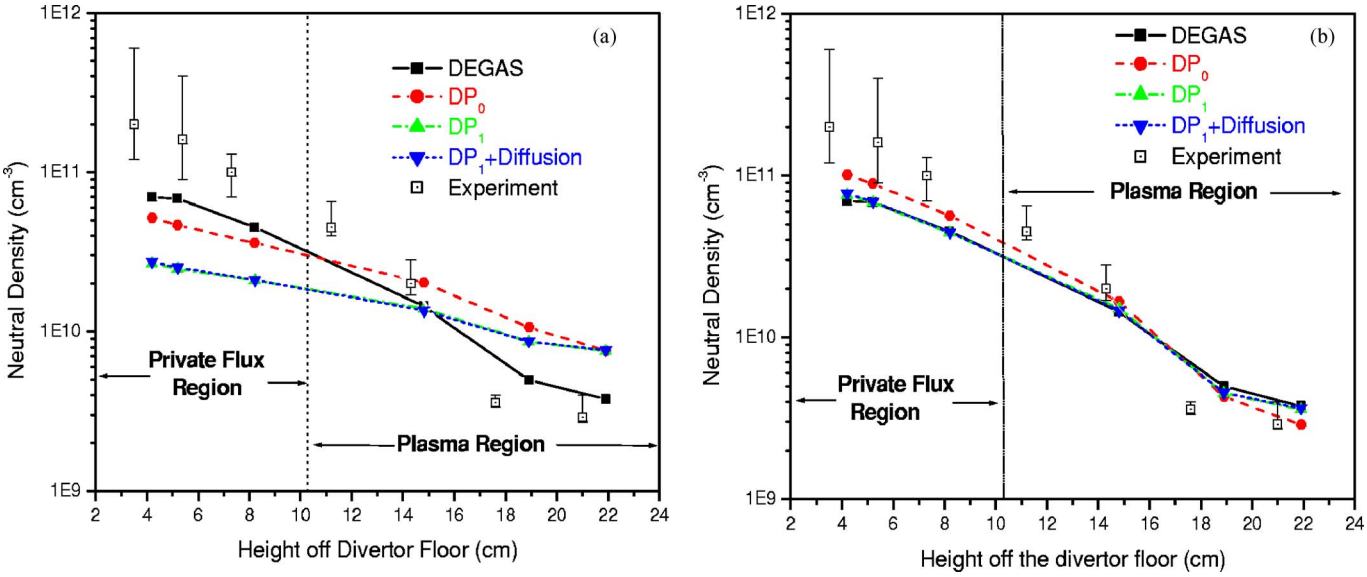

FIG. 7. (Color online) Comparison of GTNEUT and DEGAS simulations for the analysis of the DIII-D *H*-mode discharge 96747 at 3940 ms. (a) Local ion temperature approximation; (b) average neutral energy approximation.

TABLE III. CPU time (s) for the neutral analysis of DIII-D discharges.

Mode	GTNEUT	DEGAS
L	18.4	20099.6
H	35.3	15732.0

periment in the private flux region for the *H*-mode case [Figs. 7(a) and 7(b)] can be attributed to the importance of molecular effects and is explained in more detail in Ref. 4.

The CPU times required to carry out the simulations by the DEGAS and GTNEUT codes for the calculations of neutral densities in both *H* and *L* discharges are listed in the Table III, where all the calculations are performed on a SUN workstation (ULTRA-10, 360 MHz). The number of particles used in the DEGAS simulations was adjusted so that the maximum statistical error was less than 10%. It is should be mentioned that the latest version of the DEGAS code (DEGAS 2) is an order of magnitude of faster[13] than the original DEGAS code, which was used in these simulations.

VIII. CONCLUSIONS

We have extended the transmission and escape probability methodology for the calculation of neutral particle transport in magnetically confined plasmas, by developing higher order approximations which better take into account the effects of angular anisotropy, spatial nonuniformity of collision sources and energy dependence of the neutral particle distribution. The angular anisotropy of the neutral distribution function at the cell interfaces has been addressed by the implementation of a double P_1 (and higher, if necessary) approximation, whereas a finite elements-based diffusion approach has been shown to correctly account for the collision source nonuniformity on the direction of escape from short mean-free-path regions. The average neutral energy approximation has also been developed and implemented to correct the deficiencies of the original neutral energy assumption—the local ion temperature approximation—in regions of strong ion temperature gradients. These extensions have been implemented into the two-dimensional neutral transport code GTNEUT and the predictions of the upgraded code have been compared to Monte Carlo. Our model problem simulations verify the correctness of our methodology and demonstrate the increased accuracy and extended range of validity of our computational model.

[1] W. M. Stacey and J. Mandrekas, Nucl. Fusion **34**, 1384 (1994).
[2] J. Mandrekas, Comput. Phys. Commun. **161**, 36 (2004).
[3] R. Rubilar, W. M. Stacey, and J. Mandrekas, Nucl. Fusion **41**, 1003 (2001).
[4] J. Mandrekas, R. J. Colchin, W. M. Stacey, D. Zhang, and L. W. Owen, Nucl. Fusion **43**, 314 (2003).
[5] M. M. Anderson and H. C. Honeck, Proceeding of the Conference on Mathematical Models and Computational Techniques for Analysis of Nuclear Systems, Ann Arbor, 1973 (U.S. Atomic Energy Commission, Washington, D.C., 1973), Vol. 1, p. 53.
[6] R. Sanchez, Nucl. Sci. Eng. **64**, 384 (1977).
[7] D. Zhang, J. Mandrekas, and W. M. Stacey, Contrib. Plasma Phys. **44**, 45 (2004).
[8] E. E. Lewis and W. Miller, *Computational Methods of Neutron Transport* (Wiley, New York, 1984).
[9] D. Zhang, Neutral Particle Transport in Plasma Edge Using Transmission/Escape Probability (TEP) Method (Ph.D. thesis, Georgia Institute of Technology, Atlanta, GA, 2005).
[10] G. I. Bell and S. Glasstone, *Nuclear Reactor Theory* (Van Nostrand Reinhold, New York, 1970), p. 42.
[11] W. M. Stacey, *Fusion Plasma Physics* (Wiley-VCH, Berlin, 2005), p. 419.
[12] D. Zhang, J. Mandrekas, and W. M. Stacey, Contrib. Plasma Phys. (to be published).
[13] D. Stotler, Princeton Plasma Physics Laboratory (private communication, 2001).
[14] R. J. Colchin and R. Maingi *et al.*, Nucl. Fusion **40**, 175 (2000).